Archives of Dermatological Research (2025) 317:514
https://doi.org/10.1007/s00403-025-03895-8

ORIGINAL PAPER

EGFR influences the resistance to targeted therapy in BRAF ^{V600E} melanomas by regulating the ferroptosis process

Yuexin Sun[1] · Haoyue Yu[1] · Ying Zhou[1] · Jun Bao[1] · Xiaoping Qian[1,2]

Received: 26 November 2024 / Revised: 20 January 2025 / Accepted: 27 January 2025

Abstract

To identify genes differentially expressed between resistant and sensitive BRAF V600E melanoma cell lines using bioinformatics tools applied to GEO data. We retrieved and downloaded the target gene set (GSE45558) from the GEO database and used R software to filter differentially expressed genes (DEGs) between BRAF V600E melanoma cell lines resistant. The identified DEGs were subjected to GO functional enrichment analysis (including biological processes, molecular functions, and cellular components) and Kyoto Encyclopedia of Genes and Genomes (KEGG) pathway analysis, utilizing R software. Protein-protein interaction networks for the DEGs were generated using the STRING online database. Top hub genes were cross-referenced with genes related to ferroptosis from the FerrDb database to identify DEGs linked to ferroptosis in resistant melanoma cells. From the GEO database analysis, we identified the top 100 DEGs between BRAF V600E melanoma cell lines, including 50 downregulated and 50 upregulated DEGs. Using STRING and Cytoscape, we identified the top 10 hub genes: IL6, IL1B, CCL2, MMP2, TGFB2, EGFR, POSTN, SERPINE1, COL1A2, and MITF. Cross-referencing with the FerrDb database, we found that IL6 and EGFR are differentially expressed genes related to ferroptosis in resistant melanoma cells. Validation through clinical samples and in vitro experiments confirmed the high expression of the ferroptosis-related gene EGFR as a potential biomarker for resistance to targeted therapy in BRAF^{V600E} melanoma. Bioinformatics analysis identified key resistance genes in BRAF^{V600E} melanoma targeted therapy, demonstrating the impact of ferroptosis-related gene EGFR on the resistance of BRAF^{V600E} melanoma.

Keywords Ferroptosis · Differentially expressed genes · Resistance · Melanoma · Biomarkers · STRING · Cytoscape

Melanoma, a skin cancer derived from melanocytes, has not only exhibited a continuous increase in incidence but also stands as the deadliest form of skin cancer, owing to its high invasiveness and metastatic potential [1]. The treatment of melanoma remains a significant challenge in both clinical practice and research. In particular, the prevalence of BRAF gene mutations, especially the BRAFV600E mutation found in over 50% of melanoma patients, underscores the importance of investigating related therapeutic strategies [2–3]. This mutation results in the permanent activation of the BRAF protein, stimulating the MEK/ERK signaling pathway and promoting the proliferation and survival of tumor cells[4]. Initially, targeted therapies against the BRAFV600E mutation have shown promising efficacy; however, the majority of patients eventually develop resistance, leading to treatment failure. Research has identified the epidermal growth factor receptor (EGFR) as playing a critical role in the development of melanoma resistance [5–6]. EGFR, a tyrosine kinase receptor on the cell surface, whose overexpression or activation is closely associated with the development and resistance of various types of tumors [7]. Recently, ferroptosis, a novel form of non-apoptotic cell death linked to dysregulated iron metabolism and characterized by iron-dependent lipid peroxidation, has attracted extensive attention [8–9].

Yuexin Sun and Haoyue Yu They are the co-first authors,Contributed equally to this work.

✉ Jun Bao
baojun1968@sina.cn

✉ Xiaoping Qian
xiaopingqian@nju.edu.cn

[1] Department of Dermotology, Nanjing Drum Tower Hospital, Clinical College of Nanjing University of Chinese Medicine, Nanjing, Jiangsu 210000, China

[2] Department of Oncology, Nanjing Drum Tower Hospital, Clinical College of Nanjing University of Chinese Medicine, Nanjing, Jiangsu, China

Published online: 01 March 2025

Ferroptosis is emerging as a promising strategy to overcome drug resistance in cancer treatment. This form of cell death contrasts with traditional apoptosis and necrosis, presenting a unique mechanism to target cancer cells that have developed resistance to conventional therapies. While numerous studies have suggested that ferroptosis may be involved in overcoming resistance to chemotherapies and targeted therapies, its specific role and mechanisms in melanoma, particularly in BRAFV600E-mutated melanoma, remain unclear. The lack of understanding regarding how ferroptosis intersects with signaling pathways like EGFR makes this an area of critical interest. Although research on ferroptosis in cancer is burgeoning, the precise mechanisms by which it can be leveraged to counteract resistance, especially in melanoma, are still under investigation.

Given the increasing prevalence of melanoma and its resistance to current therapies, it is essential to explore novel mechanisms that may provide therapeutic strategies. This study aims to explore the mechanistic role of EGFR in melanoma, particularly how it influences resistance to BRAFV600E-targeted therapies through the regulation of the ferroptosis process [10]. By better understanding the role of EGFR in ferroptosis, we hope to uncover new opportunities for improving therapeutic outcomes in melanoma.

We hypothesize that EGFR modulates iron metabolism and ferroptosis via specific signaling pathways, thereby influencing the development of resistance in melanoma cells. To test this hypothesis, a series of cellular and molecular biology experiments will be conducted, including, but not limited to, analysis of EGFR signaling pathway activation, detection of ferroptosis-related markers, and assessment of the effects of EGFR inhibitors and ferroptosis modulators on melanoma cell survival.

Material and method

Cell culture

A375 cell were purchased from the Procell (Wuhan, China) and and maintained in Dulbeccos modified eagle medium/F12 medium with 10% fetal bovine serum and 100 µg/mL streptomycin and 100 U/mL penicillin at 37 °C with 5% CO2. The cell was cultured in Dulbecco's Modified Eagle's Medium supplemented with 10% FBS (GIBCO, Grand Island, NY), 1% penicillin-streptomycin, and 5 mM glucose at 37 °C in a humidified atmosphere of 5% CO_2. Cells were passaged at 70–80% confluence.

Construction of A375EGFR + Stable Cell Line

The A375 cell line, procured from Kaiji Biotechnology Co., Ltd. (KG148), was used to generate a stable cell line expressing human EGFR. The transfection was carried out using a lentiviral vector encoding the EGFR gene tagged with GFP, provided by Corist Biotechnology. Puromycin (Biocloud, ST551-10 mg) and Polybrene (Biocloud, C0351-1 ml) were used to enhance infection efficiency and selection. A375 cells were seeded and allowed to adhere overnight. Transfection commenced when cells reached 70% confluence. For the experimental group, polybrene was added to a final concentration of 8 µg/mL when the cell density was approximately 40%. Lentivirus was then added to the culture medium containing polybrene at an MOI of 40. Cells were selected with 0.6 µg/mL puromycin for 14 days to ensure that surviving cells were those harboring the lentiviral plasmid. Fluorescence microscopy was used to inspect and verify the expression of the EGFR overexpression plasmid. EGFR mRNA and protein levels in the stable A375EGFR + cells were quantified and validated using quantitative PCR and Western blotting, and compared with those in the normal A375 cell line to ascertain differences in EGFR expression.

Western blot

For western blotting analysis, cultured cells A375 were homogenized in RIPA lysis buffer (Thermo Fisher Scientific, catalog number: 89900). Then, the tissue or cell homogenate was centrifuged at 12,000 g (4 °C) for 0.5 h, and the supernatant was collected as protein extracts. Next, a BCA protein assay kit (Pierce™ BCA Protein Assay Kit, Thermo Fisher Scientific, catalog number: 23225) was used to measure the protein concentration. After the total proteins of fresh iced cell lysates (Human periodontal ligament fibroblasts and human bone marrow-derived macrophages) were extracted and quantified, approximately 50 µg of total proteins were loaded in an SDS/PAGE gel (Bio-Rad, catalog number: 4561096) and were transferred to a polyvinylidene fluoride membrane. Subsequently, 5% non-fat dry milk with TBS (Tris-Buffered Saline) containing 0.1% Tween-20 was used to block the nonspecific protein binding sites. After that, the bands containing target proteins were incubated with primary antibodies (Company, catalog number) overnight at 4 °C on a shaker. The following day, all bands were washed with PBS (Phosphate-Buffered Saline) three times and incubated with secondary antibodies (EGFR antibody (Novus Biologicals, NBP3-16228)) for 50 min. Finally, the bands containing target proteins were measured and quantified by the Odyssey infrared imaging system (LI-COR Biosciences). Protein expression levels were normalized to the GAPDH internal control. Finally, expose and develop the membrane for approximately 3 min in an exposure unit, with the front side of the bands facing up.

Bioinformatics analysis

Differentially expressed genes (DEGs) between BRAF V600E melanoma cell lines resistant and sensitive to targeted therapy were identified using the R programming language [11]. These genes were subjected to Gene Ontology (GO) functional enrichment analysis for biological processes, molecular functions, and cellular components, as well as Kyoto Encyclopedia of Genes and Genomes (KEGG) pathway analysis. The target sequencing gene set (GSE45558) was retrieved and downloaded from the GEO database. The STRING online platform was utilized to construct the protein-protein interaction network of the DEGs, and key hub genes were identified using Cytoscape software.

Immunohistochemistry

Clinical tissue sections were sequentially deparaffinized in xylene and rehydrated through graded ethanol. Antigen retrieval was performed using citrate buffer for 10 min. Sections were blocked with goat serum for 30 min followed by overnight incubation at 4 °C with the primary antibody. The primary antibody was discarded the next day, and the sections were incubated with the secondary antibody at room temperature, protected from light, for 1 h. After washing with buffer, diaminobenzidine (DAB) was applied to each section and allowed to incubate for 10 min before counterstaining with hematoxylin. The sections were then dehydrated, coverslipped using mounting medium, and examined under a microscope.

Survival curve analysis

Select melanomas with the BRAF V600E mutation from the TCGA database(http://gepia2.cancer-pku.cn/#index). Survival curve analysis was performed using the Kaplan-Meier method to evaluate the survival probabilities over time. All subjects were followed from the date of initial treatment until the occurrence of the event of interest or the end of the study period, whichever came first. The log-rank test was employed to compare the survival distributions between different groups [12]. Data were censored for subjects lost to follow-up or if they did not experience the event by the study's conclusion. Statistical significance was set at $p < 0.05$. The analyses were conducted using SPSS software (Version 25.0, IBM Corp., Armonk, NY, USA), and survival curves were plotted to visually depict differences between the groups.

IC50 and cell viability measurement

Experimental setup for cell groupings at 48-hour time points included: NC group (A375): human BRAFV600E melanoma A375 cells; EGFR + group (A375EGFR+): A375 cells overexpressing EGFR; treated groups NC-V and EGFR+-V with the BRAF inhibitor Vemurafenib (MCE, HY-12057); NC-T and EGFR+-T treated with the MEK inhibitor Trametinib (MCE, HY-10999); and NC-S and EGFR+-S treated with the ERK inhibitor SCH772984 (MCE, HY-50846). Cell viability and IC50 values for Vemurafenib, Trametinib, and SCH772984 in A375 and A375EGFR + cells were measured using the CCK-8 assay. Cells were seeded at 5 × 10^3 per well in a 96-well plate with six concentration groups and three replicates per dose. A control group containing only DMEM was also established with six replicates. Drug concentrations ranged from 0 to 20 μM. After 48 h of treatment, 10 μL of CCK-8 reagent was added to each well, and absorbance at 450 nm was measured after 1 h at 37 °C to calculate cell viability and determine the IC50 values for Vemurafenib, Trametinib, and SCH772984.

Intracellular labile iron measurement

Two cell groups were seeded at 1×10^6 per well in a 6-well plate and cultured for 24 h. Following this, the respective drugs were added, with each drug having three replicates, and cultured for an additional 48 h. Labile iron content within the cells was determined using an iron assay kit (Solarbio, BC5415) following the manufacturer's instructions. Absorbance was measured at 593 nm using the Thermo Multiskan Sky spectrophotometer. The standard curve was plotted using the concentrations and absorbance of the standards, and iron content was calculated relative to protein concentration.

Reduced glutathione (GSH) measurement

After 24 h of incubation, cells were treated with respective group drugs for another 48 h in a 6-well plate, each drug in three replicates. The content of reduced glutathione (GSH) was measured using a GSH assay kit (Nanjing Jiancheng, A006-2-1) according to the protocol provided. The GSH content was quantified using the Thermo Multiskan Sky spectrophotometer at an absorbance of 405 nm. The concentration of GSH was calculated relative to the protein concentration of the sample.

Result

Bioinformatics identification and correlation analysis of differentially expressed genes

Through the analysis of the GEO database, we identified the top 100 differentially expressed genes (DEGs) between BRAF V600E melanoma cell lines resistant and sensitive to targeted therapy. Among these, 50 genes were downregulated and 50 were upregulated. Using STRING and Cytoscape, we identified the top 10 hub genes: IL6, IL1B, CCL2, MMP2, TGFB2, EGFR, POSTN, SERPINE1, COL1A2, and MITF. Of these, nine genes were upregulated: IL1B, CCL2, MMP2, TGFB2, EGFR, POSTN, SERPINE1, COL1A2, and IL6; one gene was downregulated: MITF.

Using the FerrDb database, we collected genes related to ferroptosis and compared these with the top 100 differentially expressed genes identified from our initial screening. We intersected these data sets to identify differentially expressed genes related to ferroptosis in melanoma cells resistant to targeted therapy, including EGFR, GDF15, IL6, and SLC1A4. Notably, EGFR and IL6 were also among the top 10 hub genes. The presence of the BRAF V600E mutation was validated in clinical melanoma tissue samples, affirming the relevance of our gene expression findings to clinical scenarios. This validation supports the reliability of our bioinformatics and experimental approach in identifying key molecular targets in melanoma (Figs. 1 and 2).

Validation of $BRAF^{V600E}$ mutation in clinical melanoma tissue specimens

We conducted immunohistochemical (IHC) analysis on 20 cases of $BRAF^{V600E}$ melanoma tissues to detect the presence of EGFR protein. A total of 20 clinical histopathological specimens were obtained, all derived from melanoma patients confirmed to have the $BRAF^{V600E}$ mutation. Among these, five cases were resistant to targeted therapy drugs (one case to Vemurafenib and four to Trametinib) and fifteen were sensitive (three to Vemurafenib and twelve to Trametinib). The results indicated a higher accumulation of EGFR in the tissues of melanoma resistant to targeted therapy compared to those sensitive to it, with significant variations in EGFR levels observed across tumor samples. Our findings demonstrate that high expression of the ferroptosis-related gene EGFR in $BRAF^{V600E}$ melanoma could serve as a biomarker for resistance to targeted therapy. Modulating the key gene EGFR could potentially improve resistance by promoting ferroptosis in melanoma cells. (Fig. 3)

In vitro resistance validation of $A375^{EGFR+}$ cells

We engineered a stable A375 cell line overexpressing EGFR—A375EGFR+—to test resistance to three targeted therapies used in BRAFV600E melanoma: the BRAF inhibitor Vemurafenib, the MEK inhibitor Trametinib, and the ERK inhibitor SCH772984. The EGFR-overexpressing A375 cells were established using a lentiviral vector encoding human EGFR. The increased expression of EGFR was confirmed through fluorescence imaging (Fig. 4.A), RT-qPCR (Fig. 4.B), and Western blot analysis (Fig. 4.C). CCK-8 assays were conducted to determine the cell viability and IC50 of A375 and A375EGFR + cells treated with vemurafenib (BRAF inhibitor), trametinib (MEK inhibitor), and SCH772984 (ERK inhibitor). The results demonstrated that the A375EGFR + cells (EGFR overexpression group) exhibited higher IC50 values in the following treatment groups: NC-V (negative control for vemurafenib), EGFR+-V (vemurafenib treatment), NC-T (negative control for trametinib), EGFR+-T (trametinib treatment), NC-S (negative control for SCH772984), and EGFR+-S (SCH772984 treatment) compared to the A375 cells (negative control group) as shown in Fig. 4.D ($P < 0.05$).

Regulation of ferroptosis in $BRAF^{V600E}$ melanoma cells by iron death

We explored the modulation of ferroptosis in controlling resistance to targeted therapy in BRAFV600E melanoma cells and its selective efficacy in the A375EGFR + cell line using the ferroptosis inducer artesunate. The results demonstrated that artesunate significantly altered the IC50 of Vemurafenib, indicating a potential reduction in drug resistance through ferroptosis induction. Specifically, the IC50 for Vemurafenib was found to be 18.35 μM in A375 cells treated with DMSO for 8 h followed by Vemurafenib for 24 h (Fig. 5.A), and 25.94 μM in the corresponding $A375^{EGFR+}$ cells (Fig. 5.B). However, in the artesunate pre-treatment group, the IC50 values were reduced to 14.01 μM for A375 (Fig. 5.C) and 10.63 μM for $A375^{EGFR+}$ (Fig. 5.D). Notably, the IC50 was higher in both the A375 and $A375^{EGFR+}$ group treated with DMSO compared to those treated with artesunate, with statistically significant differences ($P < 0.05$).

Furthermore, using artesunate as a ferroptosis inducer on both A375 (Fig. 5A, C) and $A375^{EGFR+}$ cells (Fig. 5B, D), we observed a notable decrease in Vemurafenib IC50 values compared to the untreated groups. This reduction was more pronounced in the $A375^{EGFR+}$ cells, which exhibit higher resistance to Vemurafenib, suggesting that artesunate effectively reduces melanoma cell resistance to targeted therapy, particularly in cells with higher inherent resistance (Fig. 5.E, F).

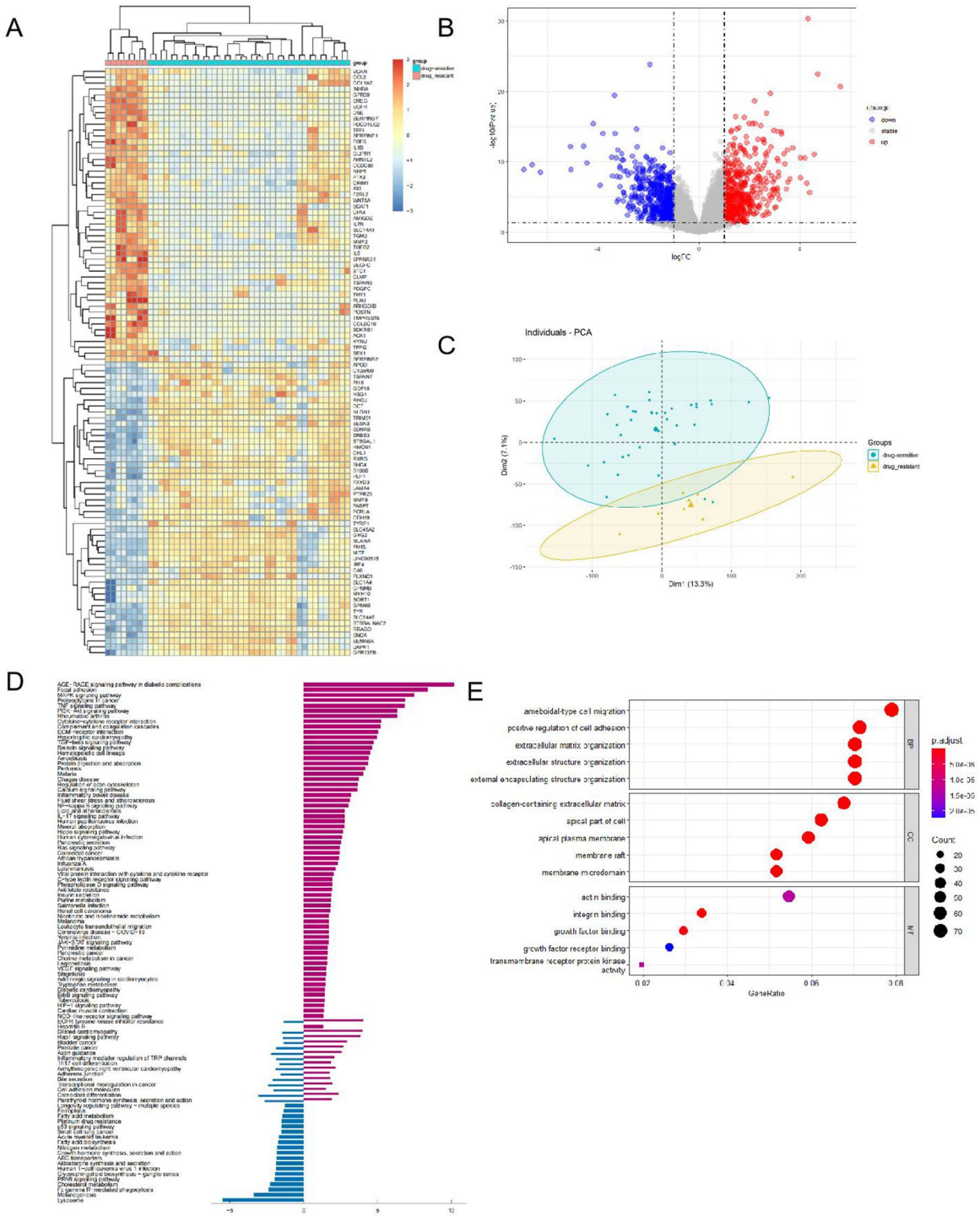

Fig. 1 Analysis of Gene Expression in BRAF V600E Melanoma. **(A)** Heatmap of the top 100 differentially expressed genes; **(B)** Volcano plot of the top 100 differentially expressed genes; **(C)** Principal Coordinate Analysis (PCA); **D.**Kyoto Encyclopedia of Genes and Genomes (KEGG) pathway analysis;**E.** Gene Ontology (GO) analysis.** $P<0.01$, compared with the Control group ($n=3$)

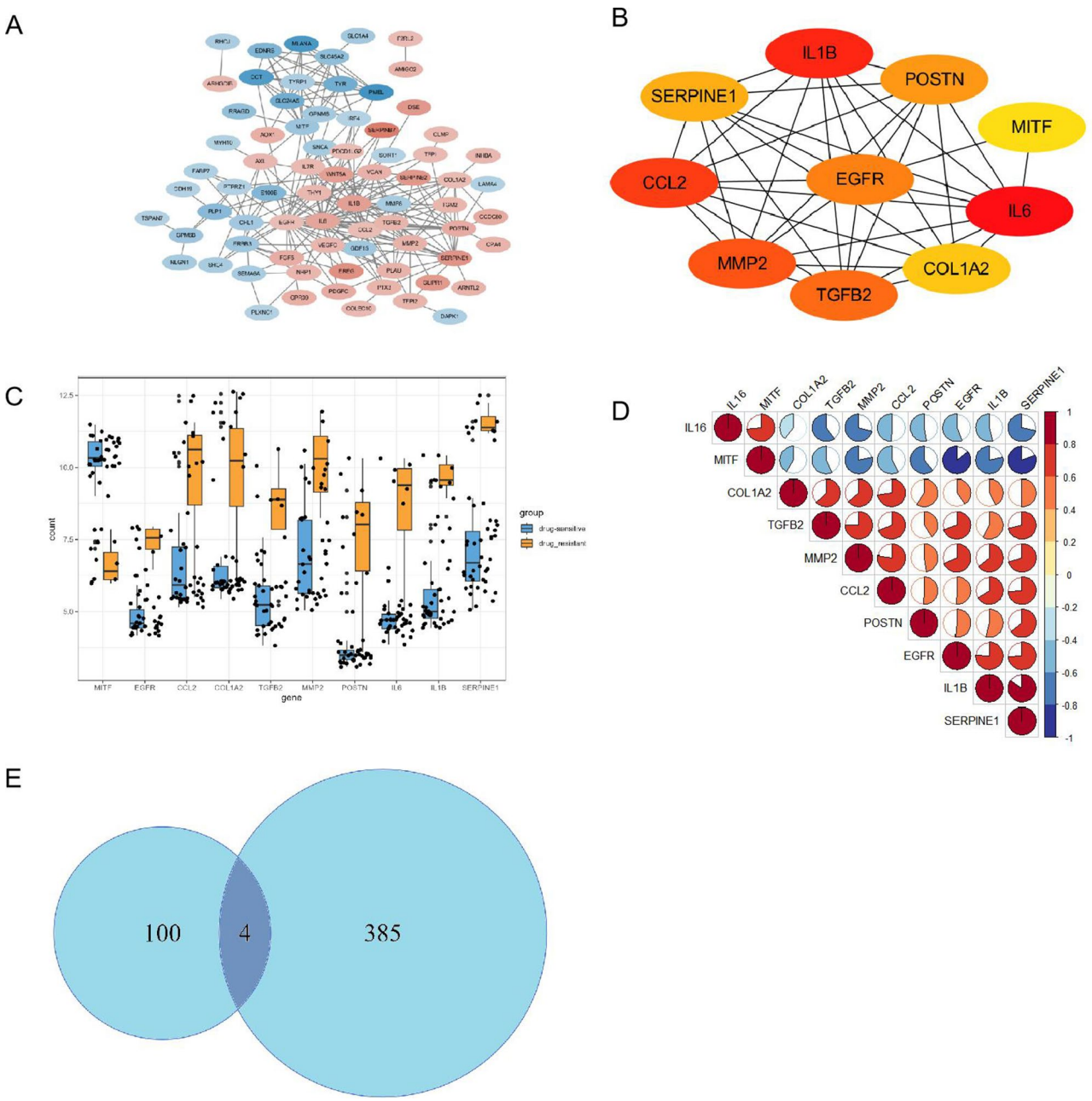

Fig. 2 Analysis of Gene and Protein Interactions in BRAF V600E Melanoma. **A.**Visualization of the protein-protein interaction network for the top 100 genes; **B.** Subnetwork analysis of the top 10 hub genes; **C.**Box plot of the top 10 hub genes; **D.** Correlation analysis of TOP10 Hub genes. **E.**Venn diagram analysis of differentially expressed genes.** $P<0.01$, compared with the Control group ($n=3$)

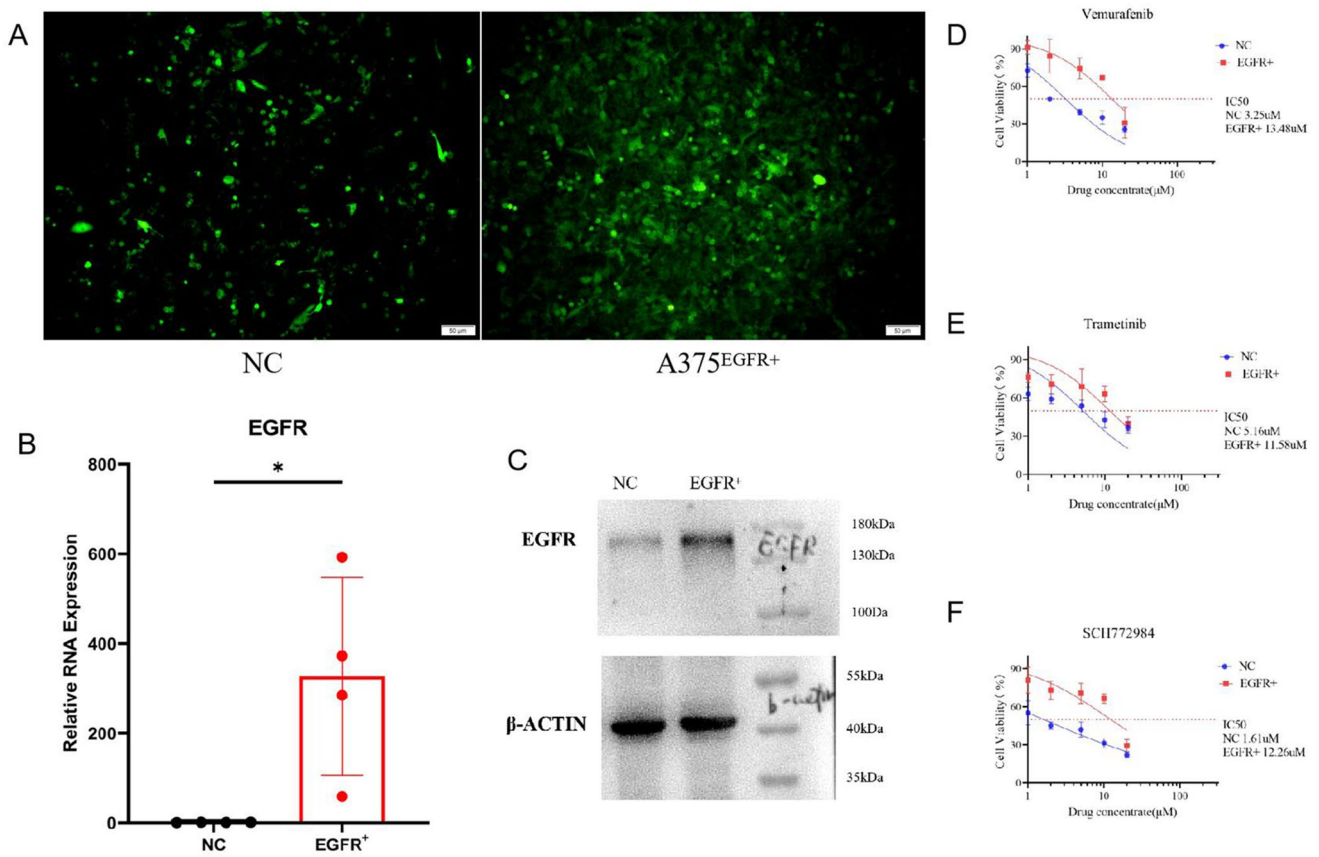

Fig. 3 Evaluation of Prognostic and Diagnostic Markers in BRAF V600E Melanoma. **A.** EGFR and IL6 survival curve analysis; **B**, **C.** Comparative analysis of EGFR immunohistochemistry between melanoma targeted therapy resistant group and sensitive group.** $P<0.01$, compared with the Control group ($n=3$)

Regulation of ferroptosis in BRAF^{V600E}mutated melanoma cells by EGFR via the NRF2/GPX4 pathway

To further investigate the specific regulatory mechanisms of EGFR, we focused on its effects on ferroptosis in BRAF^{V600E} mutated melanoma cells and the expression changes in key nodes of the NRF2/GPX4 pathway. In vitro experiments revealed that treatment with artesunate led to a significant increase in Fe^{2+} levels and a decrease in GSH levels in both A375 and A375^{EGFR+} cells (Fig. 6.A) ($P<0.05$). Moreover, the increase in Fe^{2+} and decrease in GSH were more pronounced in the EGFR-overexpressing group (Fig. 6.B) ($P<0.05$) These results indicate that A375 cells with high EGFR expression are more sensitive to ferroptosis, and the use of the ferroptosis inducer artesunate significantly reduces their resistance to Vemurafenib.

Discussion

Melanoma, particularly those cases harboring the BRAF^{V600E} mutation, presents a formidable challenge in oncological treatments due to its propensity for rapid progression and high rates of resistance to targeted therapies [13, 14]. The BRAF^{V600E} mutation activates the MEK/ERK signaling pathway, promoting tumor cell proliferation and survival [5]. Despite initial responses, resistance to BRAF inhibitors is a significant hurdle, often emerging through various adaptive mechanisms within the tumor microenvironment [15]. Recent studies have begun to explore the role of alternative cell death pathways, such as ferroptosis, a form of iron-dependent cell death, in overcoming resistance [16–17]. The focus on epidermal growth factor receptor (EGFR) as a regulator of ferroptosis introduces a novel angle in the study of melanoma resistance mechanisms. The

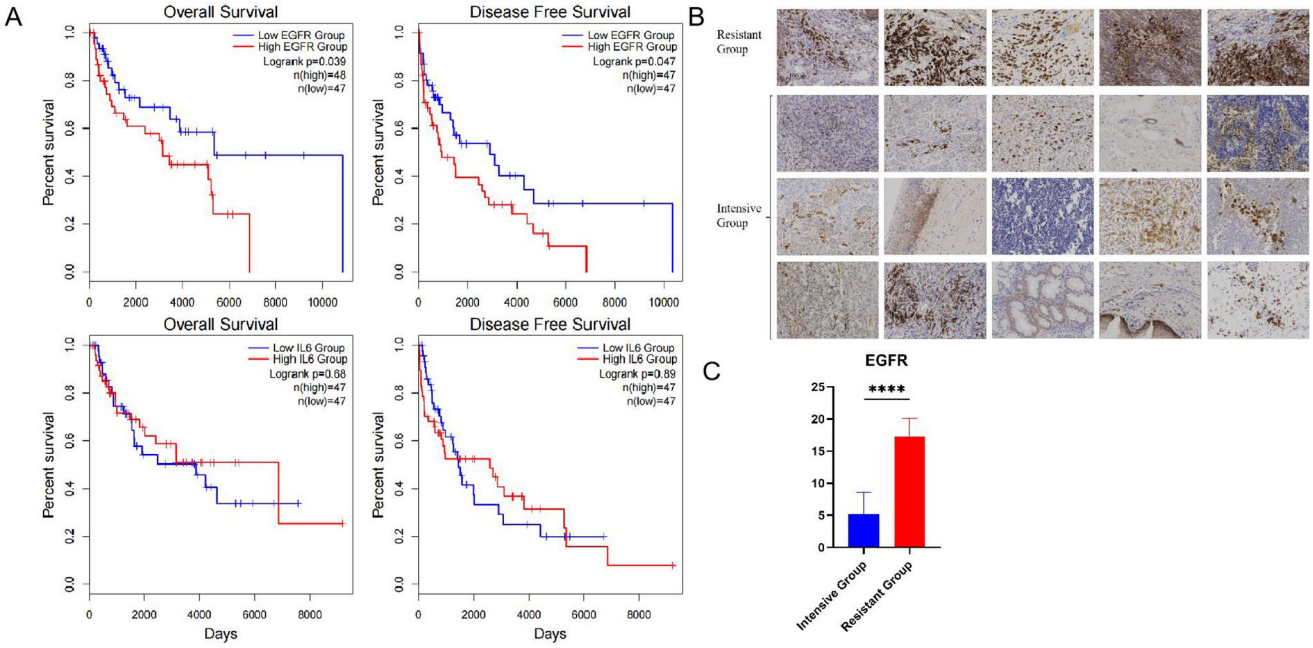

Fig. 4 Construction of A375 cells with high EGFR expression and validation of their drug resistance in vitro. **A, B,C**. High expression of EGFR was confirmed by fluorescence detection (green is GFP), PCR and Western blot (WB) in A375^{EGFR+} stable cell line, * indicates $P<0.05$; **D, E, F**.Comparison of drug resistance of A375 cells (NC group) and A375 EGFR+cells (EGFR+group) to vemurafenib, trametinib and SCH772984. *$P<0.05$.Drug response curves are shown as mean±SEM of three replicates and are representative of at least three independent experiments. NC group (A375): human BRAFV600E melanoma A375 cells; EGFR+group (A375EGFR+): A375 cells overexpressing EGFR; treated groups NC-V and EGFR+-V with the BRAF inhibitor Vemurafenib (MCE, HY-12057); NC-T and EGFR+-T treated with the MEK inhibitor Trametinib (MCE, HY-10999); and NC-S and EGFR+-S treated with the ERK inhibitor SCH772984 (MCE, HY-50846)

study concludes that EGFR plays a pivotal role in the resistance of BRAF^{V600E} melanoma cells to targeted therapies by modulating ferroptosis. Key findings indicated that ferroptosis-related genes, particularly EGFR, are differentially expressed in resistant versus sensitive cell lines [18]. Targeting EGFR to promote ferroptosis significantly mitigates resistance, suggesting a dual role for EGFR in both tumor progression and resistance via ferroptosis regulation.

The study identified EGFR as a central player in regulating ferroptosis in melanoma cells, which aligns with recent findings highlighting the receptor's broader role in cancer biology beyond its traditional signaling functions [19]. For instance, a study demonstrated that EGFR inhibition could sensitize cancer cells to ferroptosis by altering lipid metabolism pathways. These findings corroborate our results that EGFR modulation affects ferroptosis and suggest a therapeutic strategy combining EGFR inhibitors with ferroptosis inducers. The identification of differentially expressed ferroptosis-related genes, including IL6 and EGFR, in resistant melanoma cell lines provides insights into the complexity of resistance mechanisms. Research had earlier established the foundation of ferroptosis in cancer cells, highlighting its distinct biochemical features from other forms of cell death. By linking these genes to ferroptosis specifically in the context of BRAF^{V600E} melanoma, our study expands on the known landscape of cancer resistance pathways, suggesting that manipulating these genes could overcome resistance [20]. The integration of bioinformatics analysis with experimental validation strengthens the study's conclusions. This approach mirrors the methodological frameworks seen in works, which advocate for the synergistic use of computational and experimental methods to enhance the reliability of biological insights [21–21]. Our findings were robust across multiple analysis platforms and were further substantiated by in vitro experiments, thereby solidifying the role of identified DEGs in resistance mechanisms. Despite its strengths, this study has several limitations. Firstly, the reliance on in vitro models, particularly the A375 cell line, may not fully replicate the complex in vivo tumor microenvironment, potentially oversimplifying the interaction dynamics and resistance mechanisms [22]. Furthermore, the study's focus on EGFR and a limited set of ferroptosis-related genes may overlook other critical pathways involved in resistance. The gene expression profiles and the subsequent analyses are also dependent on the accuracy and comprehensiveness of the databases used, such as GEO and FerrDb, which might not encompass all relevant genes or might contain outdated annotations [23–24].

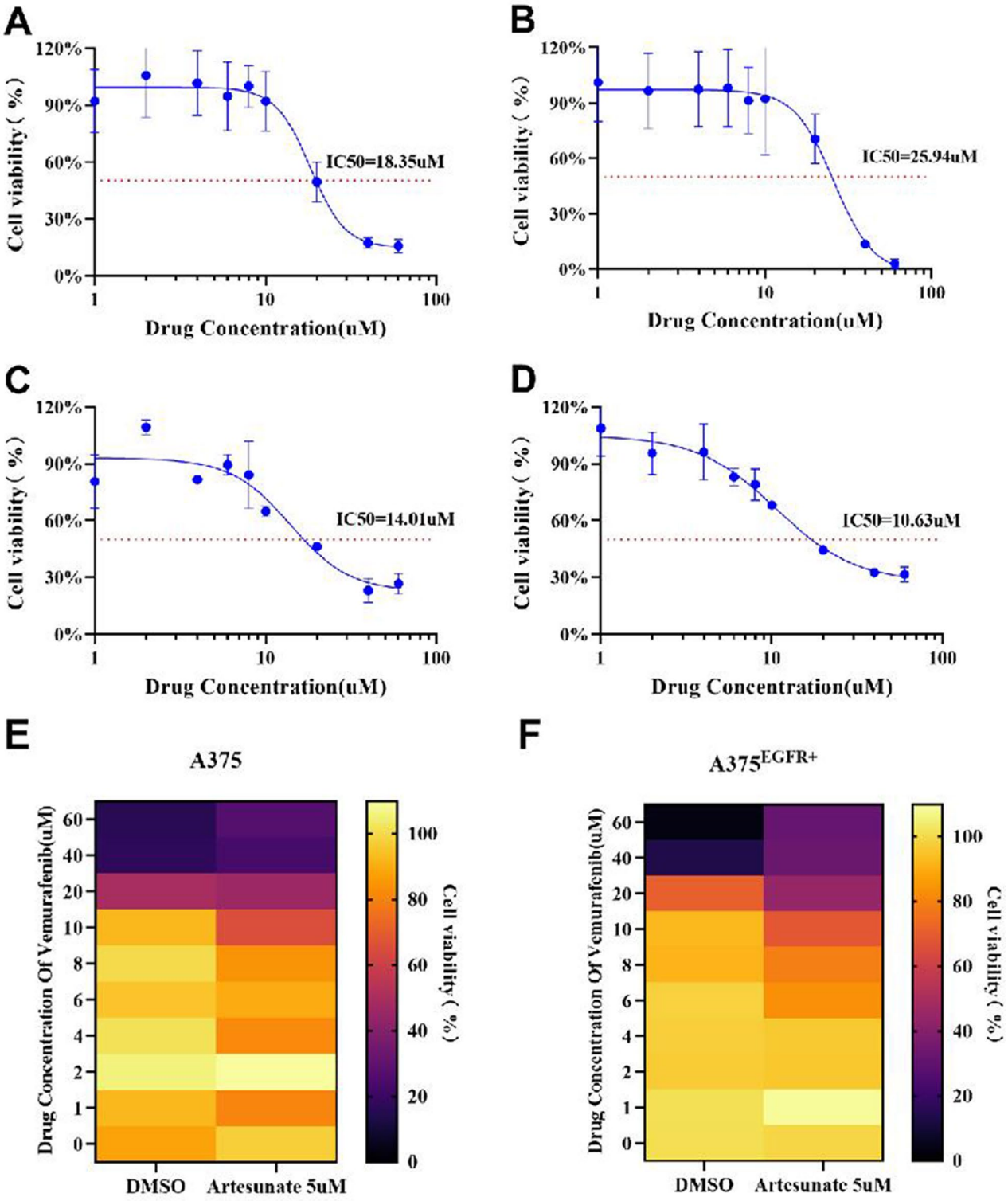

Fig. 5 Measurement of the IC50 of ferroptosis-induced BRAFV600E melanoma cells for vemurafenib. A375 and A375EGFR + cells were pretreated with DMSO and 5 μm artesunate for 8 h, respectively, to calculate the IC50 values of vemurafenib. **A**, **C.** IC50 determination for A375 cells induced with vemurafenib; **B. D.** IC50 determination for $A375^{EGFR+}$ cells induced with vemurafenib; **E.F.** Percentages of viable cells calculated relative to DMSO. Drug response curves are shown as mean ± SEM of three replicates and are representative of at least three independent experiments

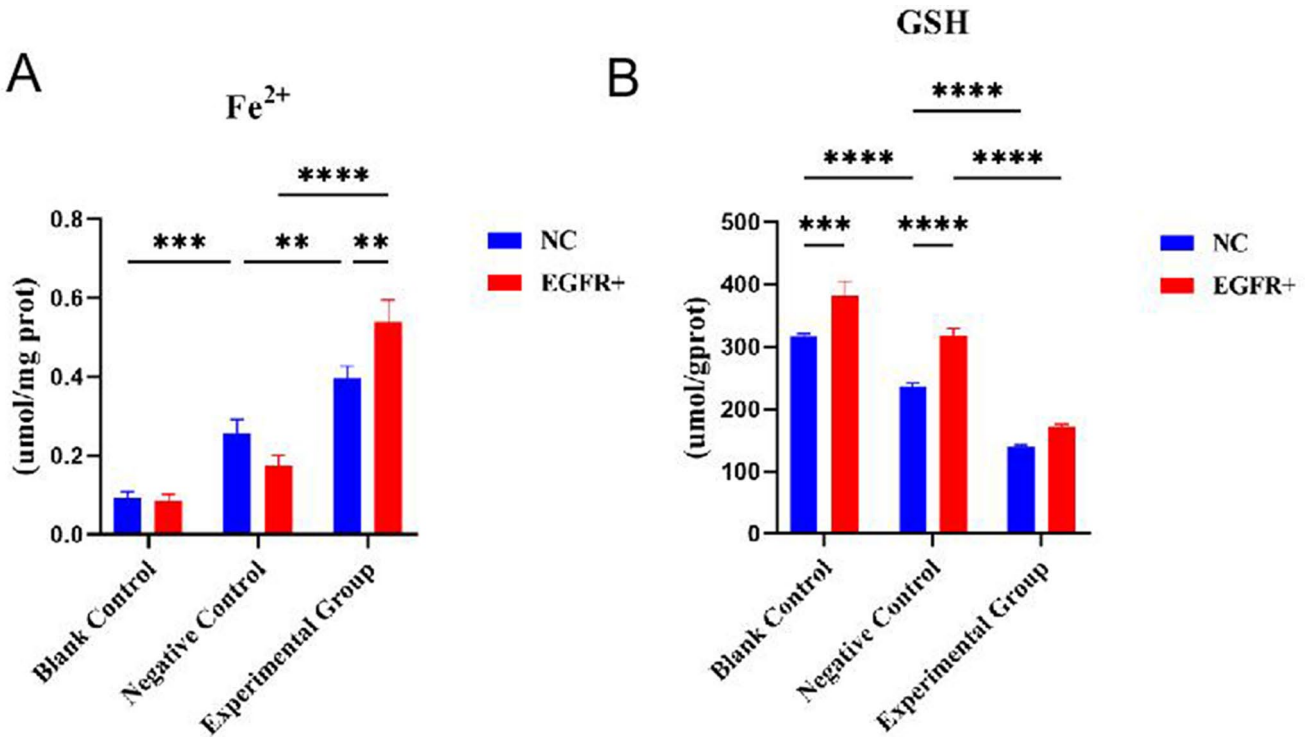

Fig. 6 Identification of $Fe^{2+}$and GSH Levels. **(A)** Measurement of Fe^{2+} levels; **(B)** Detection of GSH levels. Negative control group: BRAF inhibitor vemurafenib and DMSO treatment for 48 h (vemurafenib concentration: 5 μM). Experimental group: Vemurafenib combined with the ferroptosis inducer artemisinin hexaphenylethane for 48 h (artemisinin hexaphenylethane concentration: 10 μM). ** $P<0.01$, compared with the Control group ($n=3$)

Conclusion

In conclusion, this study provides significant insights into the role of EGFR in mediating resistance to targeted therapies in $BRAF^{V600E}$ melanoma through the regulation of ferroptosis. By highlighting the differential expression of key ferroptosis-related genes and confirming their impact through rigorous bioinformatics and experimental approaches, the research underscores the potential of targeting EGFR to enhance treatment efficacy. However, the limitations inherent in the study methodologies suggest the need for further research involving more comprehensive in vivo models and a broader spectrum of genetic analyses. Future studies should aim to elaborate on the intricate network of resistance mechanisms, exploring the synergistic effects of combining ferroptosis inducers with existing therapeutic regimes to devise more effective treatment strategies for melanoma.

Author contributions Conception and design: Yuexin SUN, Haoyue YU. Acquisition of data (provided animals, acquired and managed patients, provided facilities, etc.): Ying ZHOU. Analysis and interpretation of data (e.g. statistical analysis, biostatistics, computational analysis): Yuexin SUN, Haoyue YU. Writing, review, and/or revision of the manuscript: Yuexin SUN, Haoyue YU. Administrative, technical, or material support (i.e., reporting or organizing data, constructing databases): Jun BAO. Study supervision: Xiaoping Qian.

Funding This study was supported by Project of Institute of Chinese Medicine, Nanjing University and Aid Project of Nanjing Drum Tower Hospital Health, Education & Research Foundation, ICM2024033; the Natural Science Foundation of Nanjing University of Chinese Medicine, XZR2020056.

Data availability The experimental data used to support the findings of this study are available from the corresponding author upon request.

Declarations

Ethics approval and consent to participate This study was approved by the Medical Ethics Committee of Nanjing Drum Tower Hospital Clinical College of Nanjing University of Chinese Medicine.

Competing interests The authors declare no competing interests.

References

1. Pizzimenti S, Ribero S, Cucci MA et al (2021) Oxidative stress-related mechanisms in melanoma and in the acquired resistance to targeted therapies[J]. Antioxidants, 10(12): 1942
2. Ta N, Jiang X, Zhang Y et al (2023) Ferroptosis as a promising therapeutic strategy for melanoma[J]. Front Pharmacol 14:1252567
3. Nyakas M, Fleten KG, Haugen MH et al (2022) AXL inhibition improves BRAF-targeted treatment in melanoma[J]. Sci Rep 12(1):5076
4. Song K, Minami JK, Huang A et al (2022) Plasticity of extrachromosomal and intrachromosomal BRAF amplifications in overcoming targeted therapy dosage challenges[J]. Cancer Discov 12(4):1046–1069
5. Liu X, Zhang Y, Wu X et al (2022) Targeting ferroptosis pathway to combat therapy resistance and metastasis of cancer[J]. Front Pharmacol 13:909821
6. Castellani G, Buccarelli M, Arasi MB et al (2023) BRAF mutations in Melanoma: Biological aspects, therapeutic implications, and circulating Biomarkers[J]. Cancers 15(16):4026
7. Gao Y, Hou Q, Guo R et al (2022) Effect of Sun exposure-induced ferroptosis mechanisms on pathology and potential biological processes of primary melanoma by microarray data analysis[J]. Front Genet 13:998792
8. Massi D, Mihic-Probst D, Schadendorf D et al (2020) Dedifferentiated melanomas: Morpho-phenotypic profile, genetic reprogramming and clinical implications[J]. Cancer Treat Rev 88:102060
9. Zeng H, You C, Zhao L et al (2021) Ferroptosis-associated classifier and indicator for prognostic prediction in cutaneous melanoma[J]. Journal of Oncology, 2021: 1–16
10. Friedmann Angeli JP, Meierjohann S (2021) NRF2-dependent stress defense in tumor antioxidant control and immune evasion[J]. Pigment Cell Melanoma Res 34(2):268–279
11. Arozarena I, Wellbrock C (2019) Phenotype plasticity as enabler of melanoma progression and therapy resistance[J]. Nat Rev Cancer 19(7):377–391
12. Lorenzato A, Magrì A, Matafora V et al (2020) Vitamin C restricts the emergence of acquired resistance to EGFR-targeted therapies in colorectal cancer[J]. Cancers 12(3):685
13. Kreß JKC, Jessen C, Marquardt A et al (2021) NRF2 enables EGFR signaling in melanoma cells[J]. Int J Mol Sci 22(8):3803
14. Biersack B, Tahtamouni L, Höpfner M (2024) Role and function of receptor tyrosine kinases in BRAF Mutant Cancers[J]. Receptors 3(1):58–106
15. Shi J, Wu P, Sheng L et al (2021) Ferroptosis-related gene signature predicts the prognosis of papillary thyroid carcinoma[J]. Cancer Cell Int 21:1–14
16. Mishra R, Patel H, Yuan L et al (2018) Role of reactive oxygen species and targeted therapy in metastatic melanoma[J]. Cancer Res Front 4(1):101–130
17. Ping S, Gong R, Lei K et al (2022) Development and validation of a ferroptosis-related lncRNAs signature to predict prognosis and microenvironment for melanoma[J]. Discover Oncol 13(1):125
18. Meinert M, Jessen C, Hufnagel A et al (2024) Thiol starvation triggers melanoma state switching in an ATF4 and NRF2-dependent manner[J]. Redox Biol 70:103011
19. Shao Y, Jia H, Huang L et al (2021) An original ferroptosis-related gene signature effectively predicts the prognosis and clinical status for colorectal cancer patients[J]. Front Oncol 11:711776
20. Bebber CM, Müller F, Prieto Clemente L et al (2020) Ferroptosis cancer cell biology[J] Cancers 12(1):164
21. Meraz-Torres F, Niessner H, Plöger S et al (2024) Augmenting MEK inhibitor efficacy in BRAF wild-type melanoma: synergistic effects of disulfiram combination therapy[J]. J Experimental Clin Cancer Res 43(1):30
22. Gao W, Wang X, Zhou Y et al (2022) Autophagy, ferroptosis, pyroptosis, and necroptosis in tumor immunotherapy[J]. Signal Transduct Target Therapy 7(1):196
23. Lei ZN, Tian Q, Teng QX et al (2023) Understanding and targeting resistance mechanisms in cancer[J]. MedComm 4(3):e265
24. Mbaveng AT, Chi GF, Nguenang GS et al (2020) Cytotoxicity of a naturally occuring spirostanol saponin, progenin III, towards a broad range of cancer cell lines by induction of apoptosis, autophagy and necroptosis[J]. Chemico-Biol Interact 326:109141